

Synthesis of cross-linked polymers by reaction of sucrose and diepoxide monomers: Characterization and nuclear magnetic resonance study

G. C. Spila Riera^a, H. F. Azurmendi^b, M. E. Ramia^{b,*}, H. E. Bertorello^a and C. A. Martín^b

^a*Dpto. de Química Orgánica, Facultad de Ciencias Químicas, Universidad Nacional de Córdoba, Ciudad Universitaria, 5016 Córdoba, Argentina*

^b*Facultad de Matemática, Astronomía y Física, Universidad Nacional de Córdoba, Ciudad Universitaria, 5000 Córdoba, Argentina*

(Received 17 June 1997; revised 3 September 1997)

The synthesis of a new cross-linked structure, with sucrose and diepoxide monomers, possessing the properties of a highly swellable hydrogel polymer is reported. Characterization studies of its structure and water effects were carried out in dried and hydrated samples by CP-MAS ¹³C n.m.r., by wide-band ¹H and ²H n.m.r. and by differential thermal analysis. The results indicate that the sample is completely amorphous and disordered, that methyl groups are present and that there is strong water structuring due to hydrogen bonding, with an absence of free water at low levels of hydration. Two processes are manifest in the temperature dependence of the ²H line width. © 1998 Elsevier Science Ltd. All rights reserved.

(Keywords: cross-linked polymer; hydrogel; n.m.r.)

INTRODUCTION

Hydrophilic polymers, or hydrogels, their performance in different aqueous media and their many applications in medicine, agriculture and others, mainly owing to their biocompatibility and biodegradability, have been the object of many studies¹. Some polymers prepared using sucrose as monomer show properties of hydrogels and, because of their natural origin, compatibilities and applications in medicine are foreseen². Reactions between sucrose and epichlorohydrin³ or diepoxide^{4,5} were previously described, leading to soluble or cross-linked products with water regains of 2 to 8.

With the development of ¹³C solid nuclear magnetic resonance (n.m.r.) operating at high magnetic fields with fast Fourier transform (FFT), the technique became fundamental too for both structure and conformational studies of cross-linked insoluble polymers⁶. In addition, by means of deuterium (²H) n.m.r., the studies of water structure, deuterium motions and relaxation are possible in aqueous media doped with heavy water⁷.

In matrices of moderately hydrophilic polymers the balance between dispersive and polar interactions, especially with water, determine the structure and morphology by means of hydrogen bond interactions and the mechanism of diffusion–sorption of these molecules.

In the present work, the synthesis of a new cross-linked structure, by reaction of sucrose and 1,4-butanediol diglycidyl ether (1,4-BDE) as monomers, having the properties of a hydrogel polymer with water regain values of 30, is reported. Additionally, the characterization of its structure was carried out by scanning electron microscopy (SEM) to obtain a macroscopic picture of the grains and by

wide-band ¹H n.m.r. and cross-polarization with magic angle spinning (CP-MAS) ¹³C n.m.r. to get microscopic information; in addition, water effects studies were done by CP-MAS ¹³C and wide-band ²H n.m.r. Also, a differential thermal analysis (DTA) was done in order to observe transition enthalpy changes associated with both the phase of the hydration water and with the polymer network structure in the temperature range of interest.

EXPERIMENTAL

Sample synthesis

The synthesis of the copolymer, poly[sucrose–1,4-BDE] was realized by reacting both monomers (sucrose and 1,4-BDE) in the presence of two catalysts, sodium hydroxide and triethylamine, in an aqueous medium.

Materials

1,4-BDE, tech. 60% was obtained from Aldrich. Sucrose was provided by Fluka. 0.2 g of NaOH were dissolved in 20 ml of distilled water. Triethylamine, reagent grade, was provided by Sintorgan.

Preparation of the copolymer

A solution of 7.5 g of sucrose in 20 ml of water was prepared at 25°C. To the solution was added 12.5 ml of 1,4-BDE, 2.5 ml of triethylamine and 0.5 ml of NaOH solution. The reaction mixture was stirred for 24 h. A solid yellowish white product was obtained.

This raw product was washed exhaustively in a batch-stirred system with water, water–ethanol (50/50) and finally ethanol. The solid product obtained was dried in a vacuum system until constant weight was achieved.

* To whom correspondence should be addressed

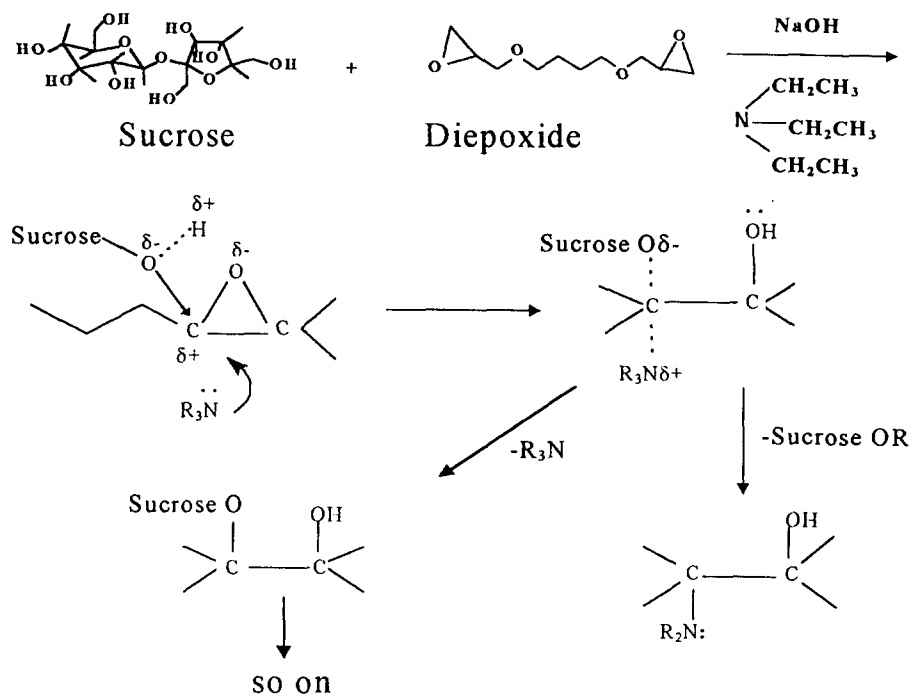


Figure 1 Mechanisms proposed for epoxy-resin curing mechanism and formation of the terminal end-capped diethylamine groups in pendant chains

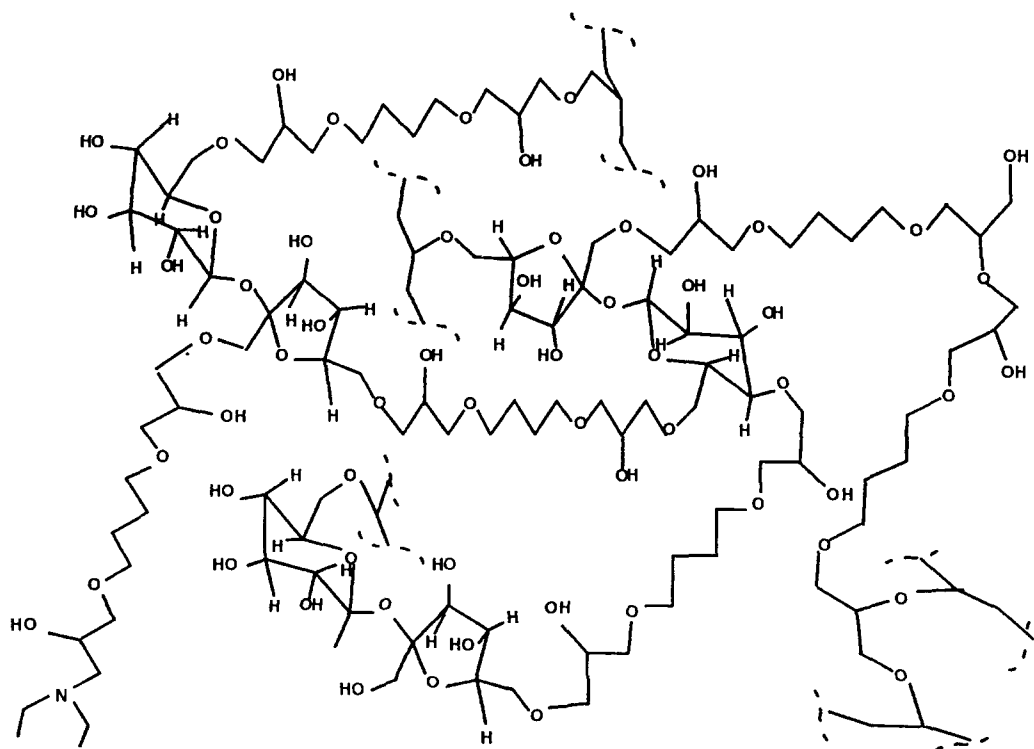


Figure 2 Scheme of cross-linked structures

In order to account for the reaction mechanism between the hydroxyl groups of sucrose and the epoxide groups, *Figure 1* gives an explanation, by means of Lewis bases, following the mechanism proposed⁸ for the epoxy-resin curing mechanism.

The reaction takes place in times of 15 to 20 h and at low temperatures, such as 25°C. The scheme depicted in *Figure 2* is intended to represent the cross-linked structures. Some

pendant chains, end-capped with diethylamine groups, as well as those with adjacent dihydroxy groups or epoxide, are also included in the depicted cross-linked structure. The presence of these groups was considered upon the characterization by ¹³C n.m.r.

The formation of the terminal end-capped diethylamine groups in pendant chains from the cross-linked macrostructure can be explained by the reaction mechanism proposed.

SAMPLE CHARACTERIZATION

N.m.r. measurements of ^{13}C , ^1H and ^2H were performed in order to characterize and determine structural information of the sample. The apparatus used was a Bruker MSL-300 with a wide-bore magnet and the probe-head was a CP-MAS 7 mm double bearing probe. The thermal stability of the sample was set and stabilized up to ± 0.1 K by a B-VT-100 Bruker temperature controller.

Special care was taken with the sample handling. Owing to its hygroscopicity, all grinding and blotting was done in a humidity-free nitrogen atmosphere. The polymer was hydrated with heavy water ($^2\text{H}_2\text{O}$) to avoid having an n.m.r. proton contribution from both the solid and the liquid.

The solid echo sequence⁹ was used for proton signal detection to obtain information about the order of crystallinity and amorphous nature of the polymer¹⁰. The 90° pulses were of $5.0 \mu\text{s}$ duration, with an echo delay of $15 \mu\text{s}$. The measurements were performed at a regulated temperature of 313 K. Greater temperatures may degrade the sample.

Prior to any ^{13}C n.m.r. measurement of the sample under study, the spectroscopy of the components was performed in order to obtain information on how the cross-linking and its dynamics affect the intensities and chemical shifts of the resonant peaks. The sample spectra were obtained by FFT of the n.m.r. signal following a standard CP-MAS pulse sequence. The MAS frequency was set to obtain its maximum value and was only limited by the sample homogeneity. Thus, its values were 2500 Hz and 1500 Hz for the dried and the hydrated polymer respectively. The CP parameters, namely the contact pulse and the ^1H 90° pulse durations, are listed in the corresponding figure captions.

In addition, to obtain information about the hydration water ($^2\text{H}_2\text{O}$), ^2H n.m.r. spectra were measured at different temperatures in the range 253–313 K for a concentration of water of 18% w/w. The relevant information was obtained from the fit parameters of the spectra, namely number of deconvolution peaks, line widths and relative intensities.

DTA measurements were carried out in the temperature range 240 to 310 K in all samples mentioned above, plus another with 88% w/w of deuterated water. The calorimeter is specially designed so that the sample holders used for CP-MAS n.m.r. could be used. This allows us to obtain the calorimetric information under the same condition as the n.m.r. data.

RESULTS AND DISCUSSION

The results of analysing the on-resonance wide line ^1H FID, on quadrature, yield the order of crystallinity of the polymer. This is due to the fact that the overall shape of the FID is the sum of the components arising from the crystalline and amorphous phases. These two components are represented by the addition of two different expressions, such that

$$M(t) = M_0^c(t) + M_0^a(t) \quad (1)$$

$$M^c(t) = M_0^c \frac{\sin(2\pi\theta t)}{2\pi\theta t} \exp\left[-\left(\frac{t}{T_c}\right)^2\right] \quad (2)$$

$$M^a(t) = M_0^{a1} \exp\left[-\left(\frac{t}{T_c'}\right)^n\right] + M_0^{a2} \exp\left(-\frac{t}{T_c''}\right) \quad (3)$$

In the above equations, equation (2) is a Gaussian profile broadened by a sine function and represents that portion of the FID that takes account of the crystalline lattice contribution. This phenomenological expression has been used successfully to describe crystalline FIDs of different solid compounds^{10,11}. The expression in equation (3) represents the amorphous contribution to the FID and it is the sum of one exponential plus a Weibullian¹² component ($\exp[-(t/T_c')^n]$), that ranges between a Lorentzian ($n = 1$) and a Gaussian ($n = 2$). Although there is no theoretical justification for the choice of the whole function, it is worth noting its election is the best that describes the experimental data. Figure 3 shows the FID of a powder sample and the theoretical fit which is achieved by means of equation (1). The parameters resulting from fitting the ^1H FID are listed in Table 1. M_0^c and M_0^a measure respectively the proportion of the crystalline and the amorphous contributions to the FID in arbitrary units. T_c , T_c' and T_c'' are inversely proportional to the line width contribution of the spectrum. The errors in the determination of all the parameters are approximately $\pm 10\%$. This is a reasonable figure considering the precision of the method; also, the fact that the fit of the data does not yield an appreciable crystalline contribution is to be considered. The credibility of such a fit lies in the fact that several fits of different FIDs, following a single 90° pulse as well as FIDs from spin echoes, yielded similar results.

Following on from the sample characterization outlined above, the ^{13}C spectra of the components of the polymer, namely sucrose and 1,4-BDE, are shown in Figure 4a and Figure 4b respectively. The sucrose spectrum is known from the literature¹³; also, the spectrum of 1,4-BDE was completely assigned. These measurements were carried out in order to provide a base for the analyses of the results obtained from the polymer, as will be seen below. Figure 5 shows the ^{13}C spectra of 300 mg of polymer (solid line). These resonant peaks are assigned in Table 2 based upon the previous spectra and on related compounds available in the literature^{14–16}. The contribution of different carbon atoms in the region between 60 and 85 ppm, arising from those modified by the polymerization process and those from the sucrose at this chemical shift, must be inferred. In addition, the peak widths are mostly impossible to determine owing to the differences in rigidity along the polymer which affect the dipolar coupling. This precluded us from providing a

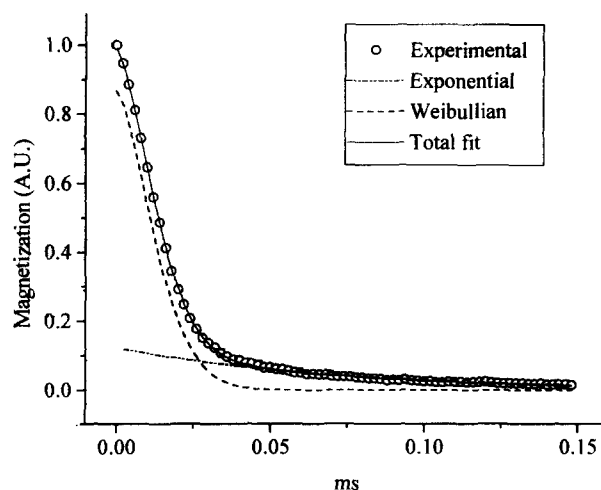


Figure 3 ^1H n.m.r. solid echo FID of 300 mg of powder sample (circles) and the theoretical fit

Table 1 Results of fitting the ^1H FID with the function described by equations (1)–(3)

M_0^s	M_0^{s1}	T_c^s (μs)	n	M_0^{s2}	T_c^{s2} (μs)
~ 0.0	0.12	15.8	1.59	0.87	70.2

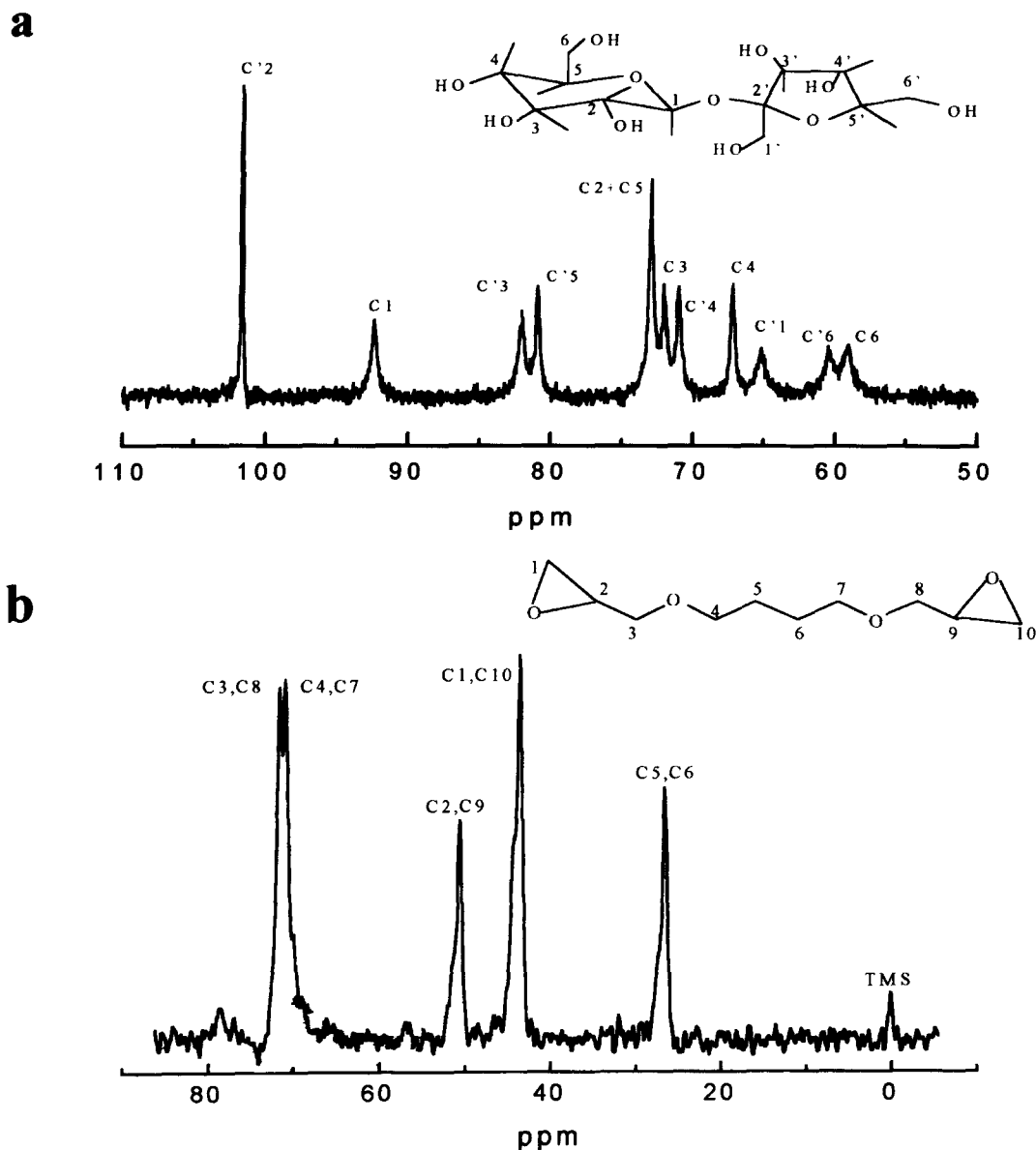


Figure 4 (a) CP-MAS ^{13}C n.m.r. spectra of solid sucrose. The 90° pulses were of $5.5 \mu\text{s}$, contact time 3.0 ms and recycle time of 15 s over 96 pulses. MAS frequencies were of 2500 Hz . (b) CP ^{13}C n.m.r. spectra of 1,4-BDE. The 90° pulses were of $6.0 \mu\text{s}$, contact time 3.0 ms and recycle time of 10 s over 64 pulses

Table 2 ^{13}C chemical shifts assignments for CP-MAS polymer spectrum; the origin of the carbon atoms is indicated in parentheses: sucrose (s), 1,4-BDE (b), triethylamine (t)

δ_c (ppm)	Assignment
103	2' (s)
91	1 (s)
82	3',5' (s)
71	2,3,5,4' (s); 1,2,3,4,7,8,9,10 (b)
65	4,1' (s)
60	6',6 (s)
53	N-CH ₂ - (t)
26	CH ₂ (b)
7	CH ₃ (t)

real deconvolution of the many contributions to the resonance peak.

The next step consisted of the hydration of the same mass of polymer with $60 \mu\text{l}$ of $^2\text{H}_2\text{O}$ (18% w/w). It is important to remark that both spectra were obtained with a contact pulse length 20% longer than that of the maximum signal cross-polarization time. In addition, it seems that $T_{1\rho}$ is little different between samples, i.e. the observed signal intensity dies away almost with the same rate as a function of the contact time. This ensures that the relative peak areas belonging to a sample spectrum may be used to obtain information¹⁶; also, a comparison of peak intensities corresponding to identical carbon atoms from the two different samples may also be done, at least qualitatively. The hydrated polymer spectrum (dashed line in Figure 5) shows a reduction of the peak intensities and a slight

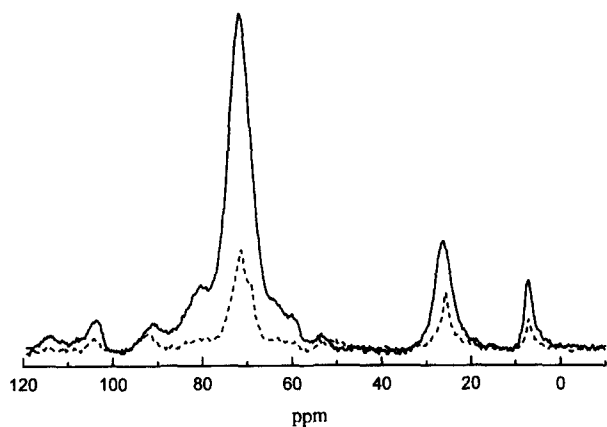


Figure 5 CP-MAS ^{13}C n.m.r. spectra of 300 mg of dried polymer (solid line) and the same sample hydrated with $60\ \mu\text{l}$ of $^2\text{H}_2\text{O}$ (dashed line). The 90° pulses were of $5.5\ \mu\text{s}$, contact time $3.0\ \text{ms}$ and recycle time of $15\ \text{s}$ over 800 pulses. MAS frequencies were of $2500\ \text{Hz}$ and $1500\ \text{Hz}$ respectively. Normal phase cycling was employed

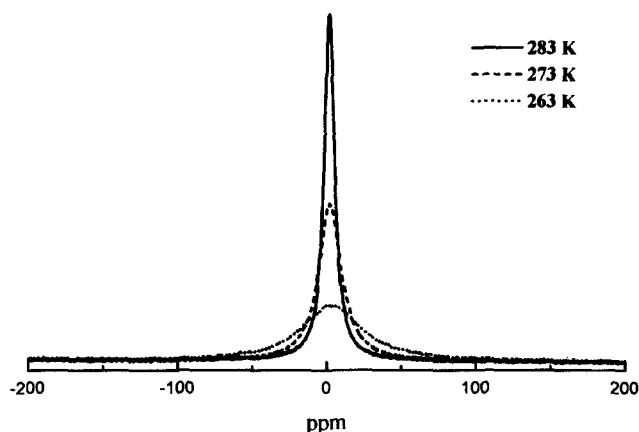


Figure 6 ^2H hydration water spectra of a sample hydrated with 18% w/w of $^2\text{H}_2\text{O}$ at three typical temperatures. The 90° pulses were of $9.5\ \mu\text{s}$ and recycle time of $1\ \text{s}$ over 32 pulses. MAS frequency was $1500\ \text{Hz}$

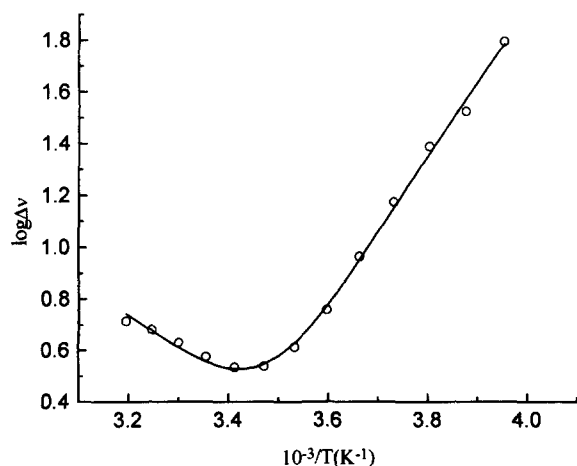


Figure 7 Arrhenius plot showing the biexponential behaviour of the hydrated sample

reduction of the line widths, rendering the appearance of some structure in the peaks. In summary, both spectra are very similar, except for the relative intensities between peaks.

Finally, the ^2H spectra of the hydration water were measured in the temperature range from 253 to $313\ \text{K}$. *Figure 6* shows the spectra at three typical temperatures. All the resonance lines correspond to single Lorentzian profiles, whose widths vary with temperature.

Figure 7 depicts the temperature behaviour of the ^2H line width in an Arrhenius plot ($\log \Delta\nu(T)$ versus $1/T$). The experimental points are well fitted by a double exponential function; therefore, it is possible to assume the existence of two superimposed mechanisms, acting in all the temperature range with opposite effects upon the dipolar Hamiltonian, which governs the line width. Each mechanism is dominant at different temperatures and follows an Arrhenius-type function. Since it is possible to characterize each range of temperature, namely (a) between 253 to $283\ \text{K}$ and (b) 293 to $313\ \text{K}$, by an activation energy E , then

$$\Delta\nu(T) \propto \tau_0 \exp\left(-\frac{E_a}{RT}\right) + A \exp\left(\frac{E_b}{RT}\right) \quad (4)$$

where R is the gas constant. In writing equation (4) it has been assumed that the line width drop is driven by motional narrowing characterized by a period of oscillation $\tau(T)$ with activation energy E_a . The second term of equation (4) describes the increase of $\Delta\nu(T)$ in the higher temperature range. The values of the activation energies are

$$E_a = 23.5\ \text{kJ mol}^{-1} \quad E_b = 7.1\ \text{kJ mol}^{-1}$$

Notice that the value of E_a obtained is typical of a hydrogen bond in organic compounds¹⁷; therefore $\tau(T)$, the first term of equation (4), is the period of oscillation of such a bond. In order to account for the second term of equation (4) we assume that, as the sample temperature increases, the polymer chains become progressively untangled, thus allowing an approach of the water molecules and, consequently, a reduction of the distance between deuterium and hydrogen atoms of the chains. Such a mechanism will produce an increase of the dipolar interaction, and the dipole-dipole distance behaves in temperature as

$$d_{\text{H},^2\text{H}} = d_0 \exp\left(-\frac{E_b}{kT}\right) \quad (5)$$

On these grounds, the second term coefficient of equation (4) is $A \propto d_0^{-3}$, and $E_b = 3E_b'$.

The calorimetric information obtained by DTA gives the enthalpy changes associated with phase transitions. For this particular case, three samples, pure polymer with 0%, 18% and 88% w/w ($160\ \mu\text{l}$) of heavy water mass, were analysed. *Figure 8a,b* shows the thermal evolution of the 18% w/w sample and that of $60\ \mu\text{l}$ of heavy water in the range 240 to $310\ \text{K}$. The hydrated polymer curve almost fits the base line of the graph and no transition peak is observed at $276.97\ \text{K}$, which is the free heavy water solid-to-liquid phase transition temperature. It has been shown in DTA that the area under the thermal evolution as a function of time $\Delta T(t)$, under proper conditions, is directly proportional to the mass of free water undergoing the transition¹⁸. Therefore, in the 18% w/w of hydration no free water is observed in the polymer. In addition, a small hump is observed at approximately $260\ \text{K}$, *Figure 8b*, which is associated with a premelting effect induced by the presence of water in the polymer.

Figure 9 shows the thermal evolution of both the sample hydrated up to 88% w/w and that of $160\ \mu\text{l}$ of heavy water. The graph corresponding to the polymer is qualitatively similar to a superposition of the evolutions of *Figure 8*,

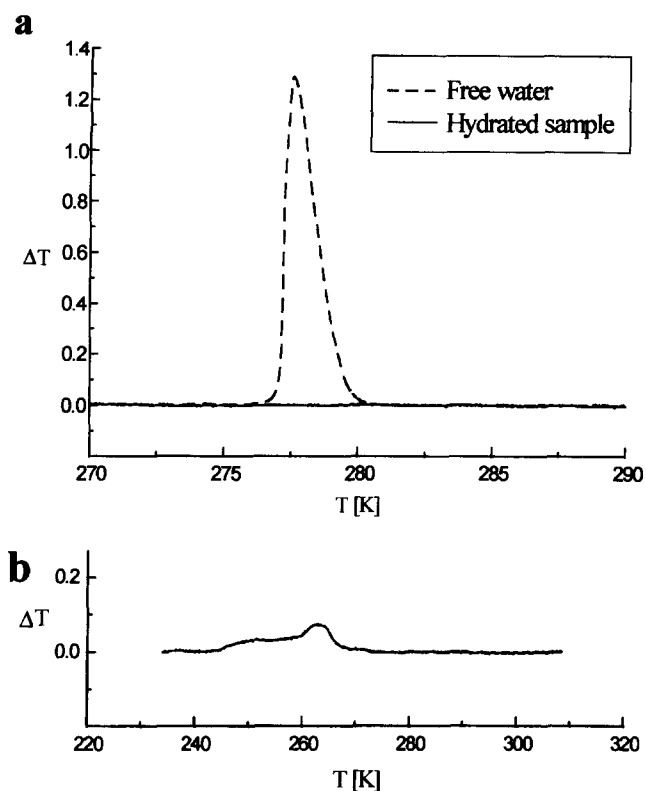


Figure 8 (a) DTA of the sample with 18% w/w of $^2\text{H}_2\text{O}$ and $60 \mu\text{l}$ of free $^2\text{H}_2\text{O}$. No transition is observed at melting point in the sample. (b) A small transition occurs in the hydrated sample between 245 and 270 K whose area is 10% of the same mass of free water

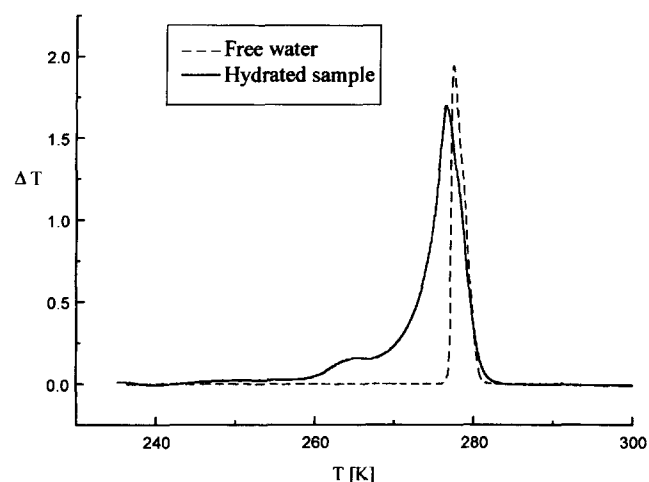


Figure 9 DTA of the sample with 88% w/w of $^2\text{H}_2\text{O}$ and the same mass of free water. In this case the ratio between the respective areas is 0.9. The transition between 245 and 270 K remains present

except that the premelting effect is amplified by the existence of more water in the sample. A difference between the areas representing $\Delta T(t)$, for the sample hydrated up to 88% w/w and that of $160 \mu\text{l}$, gives the amount of structured water, as measured by DTA. The results show that, within the sensitivity of the technique, the polymer structures 18% w/w with an error of 2% w/w. This error is produced in the determination of the area under the transition peak, which is broadened by the existence, in the

hydrated polymer, of an interface of quasi-structured water between free and structured water.

CONCLUSION

The analysis of the ^1H n.m.r. FID indicates that the sample, within the experimental errors, is completely amorphous and disordered; this is based on the fact that the coefficient M_0^c is approximately 1% of M_0^a . This is consistent with the picture obtained by SEM, *Figure 10*. In addition, the profiles of the ^2H spectra in the sample with 18% w/w water (*Figure 6*) are single Lorentzian. This would not be possible if the structure was ordered. Also, several trials to obtain an X-ray pattern were unsuccessful.

^{13}C n.m.r. spectra, of both the pure polymer and the hydrated one, show a resonant peak at 7 ppm which is not present in the spectra of the polymer components. This peak is due to carbon atoms of cap-ended chains of diethylamino groups, which arise from a secondary reaction between the catalyst, triethylamine, and the epoxy groups (see *Figure 2*). The rest of the peaks are well assigned.

The hydration of the same mass of polymer, with heavy water, shows a reduction of the ^{13}C peaks intensities and a slight line narrowing. This may be due to the low hydration of the polymer that produces a small motional incremental which averages out the dipolar interaction between ^{13}C and ^1H nuclei, which is evidenced by the appearance of a slight narrowing in the resonance lines. Also, the existence of hydrogen bonding may cause exchange of the hydrogen of the hydroxyl groups by deuterium atoms of the bulk water, producing an additional reduction of the ^{13}C intensities.

The analysis of the deuterium spectra at various temperatures reflects the existence of two line-width narrowing mechanisms with activation energies $E_a \approx 24 \text{ kJ mol}^{-1}$ (for temperatures less than 283 K) and $E_b \approx 7 \text{ kJ mol}^{-1}$ (for temperatures greater than 293 K). The first figure is in the range of hydrogen bond activation energies. The second may be due to progressive re-arrangement of water, produced by an untangling of the polymer chains, that makes the dipolar interaction more effective. This interesting behaviour will be the subject of a detailed study in future work.

DTA measurements shows that for an hydration of 18% w/w the water remains structured, whereas for an hydration of 88% w/w the appearance of a large amount of free water is clear. The calorimetry reveals that the polymer structures



Figure 10 SEM of dried polymer. Magnification factor 2500 (scale mark is $10 \mu\text{m}$)

up to about 18% of the total mass of added water. Therefore, for the same mass of polymer as that in the previous case, the volume of structured water is about 110 μl .

ACKNOWLEDGEMENTS

This work was partially supported by CONICET, CONICOR, SECYT-UNC and Dpto. de Física, Universidad Nacional del Sur.

REFERENCES

1. Glass, J. E., *Hydrophilic Polymers*, ACS Series 248. ACS, Washington, DC, 1996.
2. Pastoriza, M. A. and Bertorello, H. E., *Polymer Bull.*, 1986, **15**, 241.
3. Flodin, P. T., *Dextran Gels and their Applications in Gel Filtration*. Pharmacia, Uppsala, Sweden, 1962, p. 21.
4. Cohen, S. G. and Haas, H. C., *J. Am. Chem. Soc.*, 1953, **47**, 1733.
5. Carosino, L. and Clayton, A. B., US Patent 5319048 A 940607.
6. Buchholz, F. L. and Peppas, N. A., *Superabsorbent Polymers*, ACS Series 573. ACS, Washington, DC, 1994, p. 4.
7. Davis, J. H., *Biochem. Biophys. Acta*, 1983, **737**, 117.
8. Lee, H. and Neville, K., *Handbook of Epoxy Resins*. MacGraw Hill, New York, 1967, p. 4.
9. Powels, J. G. and Strange, J. H., *Proc. Phys. Soc.*, 1963, **11**, 431.
10. Dadayli, D., Harris, R. K., Kenwright, A. M., Say, B. J. and Sünnetçioğlu, M. M., *Polymer*, 1994, **35**, 4083.
11. Abragam, A., *Principles of Nuclear Magnetism*. Oxford University Press, Oxford, 1961, p. 120.
12. Weibull, W., *J. Appl. Mech.*, 1951, **18**, 293.
13. Sherwood, M. H., Alderman, D. W. and Grant, D. M., *J. Magn. Res. A*, 1992, **104**, 132.
14. Fumitaka, H., *Nuclear Magnetic Resonance in Agriculture*, ed. P. E. Pfeffer and W. V. Gerasimowicz. CRC Press, Boca Raton, FL, 1988, Chapter 10.
15. Cudby, M. E. A., Harris, R. K., Metcalfe, K., packer, K. J. and Smith, P. W. R., *Polymer*, 1985, **26**, 169.
16. Voelkel, R., *Angew. Chem. Int. Ed. Engl.*, 1988, **27**, 1468.
17. Wade, L. G., Jr, *Química Orgánica*, second edition. Prentice-Hall Hispanoamérica, S.A., México, 1993, p. 64.
18. Wunderlich, B., *Thermal Analysis*. Academic Press, San Diego, 1990, p. 158.